THE JOURNAL OF PHYSICAL CHEMISTRY B

Article

pubs.acs.org/JPCB

# Effect of PEGylation on Drug Entry into Lipid Bilayer

Sami Rissanen,[†] Marta Kumorek,[‡] Hector Martinez-Seara,[†] Yen-Chin Li,[§] Dorota Jamróz,[‡] Alex Bunker,[§] Maria Nowakowska,[‡] Ilpo Vattulainen,[†,∥] Mariusz Kepczynski,*[,‡] and Tomasz Róg*[,†]

[†]Department of Physics, Tampere University of Technology, PO Box 692, FI-33101 Tampere, Finland

[‡]Faculty of Chemistry, Jagiellonian University, Ingardena 3, 30-060 Kraków, Poland

[§]Centre for Drug Research, Faculty of Pharmacy, University of Helsinki, FI-00014 Helsinki, Finland

[∥]MEMPHYS—Center for Biomembrane Physics, University of Southern Denmark, DK-5230 Odense, Denmark

Supporting Information

**ABSTRACT:** Poly(ethylene glycol) (PEG) is a polymer commonly used for functionalization of drug molecules to increase their bloodstream lifetime, hence efficacy. However, the interactions between the PEGylated drugs and biomembranes are not clearly understood. In this study, we employed atomic-scale molecular dynamics (MD) simulations to consider the behavior of two drug molecules functionalized with PEG (tetraphenylporphyrin used in cancer phototherapy and biochanin A belonging to the isoflavone family) in the presence of a lipid bilayer. The commonly held view is that functionalization of a drug molecule with a polymer acts as an entropic barrier, inhibiting the penetration of the drug molecule through a cell membrane. Our results indicate that in the bloodstream there is an additional source of electrostatic repulsive interactions between the PEGylated drugs and the lipid bilayer. Both the PEG chain and lipids can bind $Na^+$ ions, thus effectively becoming positively charged molecules. This leads to an extra repulsive effect resulting from the presence of salt in the bloodstream. Thus, our study sheds further light on the role of PEG in drug delivery.

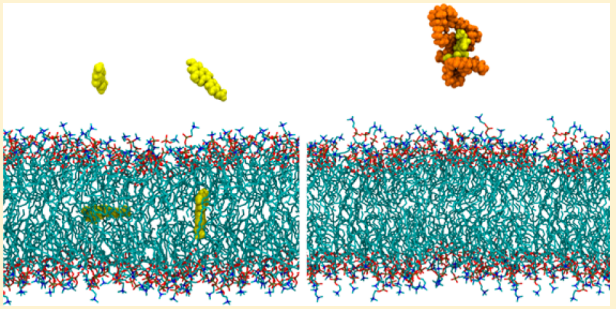

## 1. INTRODUCTION

Poly(ethylene glycol) (PEG) plays an important role in drug delivery. It is used as a protective coating material for drug delivery carriers, such as liposomes[1] and nanoparticles.[2] A similar protective effect may be achieved for individual drug molecules through the covalent attachment of a single PEG chain, called PEGylation. This has been used effectively for proteins[3] and some other drug molecules.[4,5] The protective properties of PEG are due to its action as a "stealth shield", inhibiting the drug uptake by cells of the immune system like macrophages, thus increasing its bloodstream lifetime. For example, the PEGylation of liposomes increases their bloodstream lifetime from ∼1 h to 1−2 days.[6] The effectiveness of PEG in this protective role results from its specific properties. It is soluble in organic solvents as well as in water, it is nontoxic, and it can be eliminated from the body through a combination of both renal and hepatic pathways.[7] It also exhibits protein resistance and non-immunogenicity, and it has one of the lowest levels of protein or cellular absorption of any known polymer.[8] It is believed that these unusual properties of PEG may, in part, be due to its highly hydrated polyether backbone, which is a capable acceptor in hydrogen bond formation, resulting in a large excluded volume.

PEG-functionalized porphyrins and their analogues are being considered for use as effective photosensitizers in photodynamic therapy (PDT) of malignancies and some other diseases. Several PEG conjugates of chlorins[9,10] and porphyrins[11−13] have been developed and studied *in vitro* and *in vivo*. Hornung et al. studied a derivative of meso-tetra(hydroxyphenyl)chlorin (m-THPC) *in vivo* with four long (2000 Da) PEG side chains.[9] They demonstrated highly selective targeting of cancer cells by this compound in a rat ovarian cancer model. Grahn et al. investigated m-THPC modified with 1−3 PEG chains of two different molecular weights (2000 and 5000 Da).[10] Their *in vivo* studies showed that the length of the PEG chain had relatively little effect on the patterns of bioactivity. Lottner et al. proposed a potential photosensitizer for PDT based on hematoporphyrin or tetraarylporphyrin−platinum(II) complex with two or three PEG fragments bound to a porphyrin core.[11,12] Nawalany et al. studied a series of 5,10,15,20-tetrakis(4-hydroxyphenyl)-porphyrin (p-THPP) derivatives bearing one PEG chain with a molecular weight of 350, 2000, or 5000 Da.[13] They showed that the attachment of the polymer resulted in a pronounced reduction of the dark cytotoxicity of the parent porphyrin, and that the derivative with PEG of 2000 Da molecular weight (∼45 units) has the highest photodynamic efficacy for cancer cell lines.

**Received:** October 25, 2013
**Revised:** December 18, 2013
**Published:** December 18, 2013

Biochanin A, 5,7-dihydroxy-4′-methoxyisoflavone (BIOCH), belongs to the isoflavones, which are a large class of polyphenolic compounds naturally occurring in a wide range of plants, fruits, vegetables, and herbs. The isoflavones are of great interest in pharmaceutical and medical studies due to their beneficial properties as antioxidative,[14] antibacterial,[15] and anticancer agents.[16] Although isoflavones show various modes of biological activity, they also have some drawbacks, including poor solubility in water, aggregation, low efficiency of accumulation in cells and tissues, and fast biotransformation into inactive metabolites *in vivo*.[17] Therefore, many efforts have been undertaken to overcome the above-mentioned problems. The isoflavones have been subjected to various chemical modifications, e.g., conjugation with peptide ligands,[18] fatty acid chains,[19] sugar moieties,[20] or substitution of fluoro, methoxyl, or amino groups.[21] In some cases, the novel derivatives of isoflavones have shown improved biological activities in comparison to the parent compounds.

In this article, we present the results of atomic-scale molecular dynamics (MD) simulations on the interactions between two PEGylated drug molecules, p-THPP and BIOCH (see Figure 1), and a model membrane. First, we consider the behavior of the PEGylated drugs solvated in water at physiological salt concentration (140 mM). Next, the PEGylated molecules are considered on the surface of a 1-palmitoyl-2-oleoylphosphatidylcholine (POPC) bilayer. Systems with and without salt are explored to study the effect of sodium ions on the penetration of the PEGylated molecules to the bilayer. Finally, for comparison, we consider the behavior of the non-PEGylated BIOCH or p-THPP molecules in the presence of the POPC bilayer.

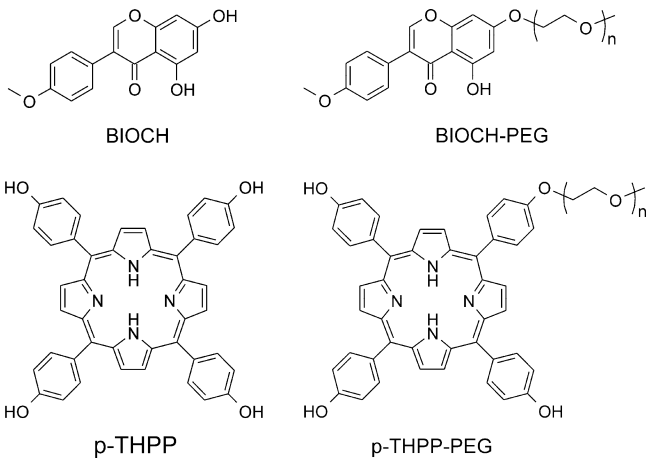


**Figure 1.** Chemical structures of BIOCH and p-THPP and their pegylated derivatives BIOCH-PEG and p-THPP-PEG.

In addition to the protective effect of PEG, functionalization of a drug molecule with a polymer is known to act as an entropic barrier for its penetration into a cell membrane.[22] Our results show that in the case of PEG this effect is strengthened by additional electrostatic interactions resulting from the strong association of $Na^+$ ions to both the plasma membrane and the PEG chain itself. Thus, the additional electrostatic as well as entropic repulsion occurs between the PEGylated drug molecule and a cell membrane. This effect is accentuated by salt that is present in natural blood plasma.

## 2. METHODS

In this study, we performed atomistic MD simulations for six model systems. The chemical structures of all the molecules considered in these studies are shown in Figure 1. The simulations for each system were repeated several times, and a summary of the studied systems is given in Table 1. Two systems contained one molecule of p-THPP (system 1) or BIOCH (system 2) with the covalently attached PEG chain of length 45 units (p-THPP-PEG or BIOCH-PEG) dissolved in water. The systems were constructed similarly to our previous studies[23] and were hydrated with ∼11 200 water molecules. Then, $Na^+$ and $Cl^-$ ions were added (corresponding to a concentration of 140 mM) for simulations that were 100 ns long. As a control, similar systems without salt were simulated for 300 ns. In addition, two systems containing one molecule of p-THPP-PEG (system 3) or BIOCH-PEG (system 4) initially placed at the lipid bilayer interface were also simulated. In these systems, where the initial structures of lipid bilayers were taken from our previous studies,[24] the lipid bilayer was composed of 128 POPC molecules and was hydrated with ∼7800 water molecules. Twenty $Na^+$ and $Cl^-$ ions were added (corresponding to a concentration of 140 mM). These simulations were repeated five times using different initial conformations of p-THPP-PEG or BIOCH-PEG molecules, randomly chosen from the simulated systems 1 or 2. All simulations were 200 ns long. As a control, similar systems without salt were simulated for 1000 ns. The last two systems, simulated over a period of 200 ns, contained four molecules of p-THPP or BIOCH placed at or in the POPC bilayer. The snapshots of the initial structure and the structures at the end of the simulations are shown in Figure 2.

Lipids, p-THPP, BIOCH, PEG molecules, and ions were parametrized using the all-atom OPLS force field.[25−29] Details of force-field implementation and partial charge choice can be

**Table 1. Summary of the Studied Systems**

| | system 1 | system 2 | system 3 | system 4 | system 5 | system 6 |
|---|---|---|---|---|---|---|
| molecule | P-Thpp-Peg | Bioch-Peg | P-Thpp-Peg | Bioch-Peg | P-Thpp | Bioch |
| number of molecules | 1 | 1 | 1 | 1 | 4 | 4 |
| water | 11200 | 11250 | 7800 | 7800 | 7800 | 7800 |
| $Na^+$ | 28 | 29 | 20 | 20 | 20 | 20 |
| $Cl^-$ | 28 | 29 | 20 | 20 | 20 | 20 |
| POPC | | | 128 | 128 | 128 | 128 |
| no. of repeats | 15 × 100 ns[a]<br>1 × 300 ns[b] | 8 × 100 ns[a]<br>1 × 300 ns[b] | 5 × 200 ns[a]<br>1 × 1000 ns[b] | 5 × 200 ns[a]<br>1 × 1000 ns[b] | 3 × 200 ns[a] | 2 × 200 ns[a] |

[a]Number of repeats and simulation length with salt. [b]Number of repeats and simulation length without salt; in these cases, the systems did not include $Na^+$ and $Cl^-$ ions.


dx.doi.org/10.1021/jp4105745 | J. Phys. Chem. B 2014, 118, 144−151

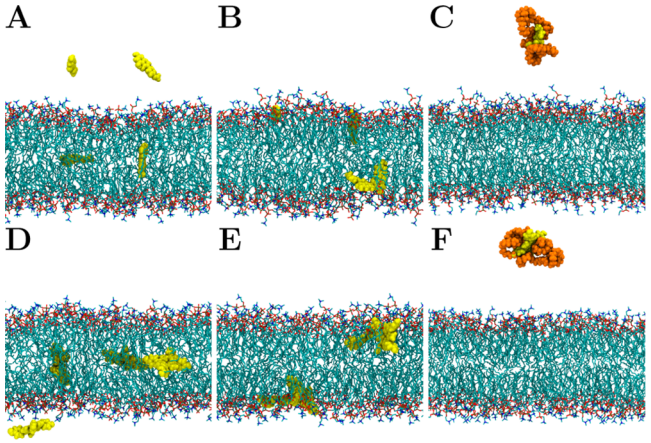


**Figure 2.** Snapshots of the configurations at $t$ = 0 and 200 ns for (A, B) BIOCH and (D, E) p-THPP, in respective order. (C) A snapshot of the configuration at $t$ = 100 ns for BIOCH-PEG. (F) A snapshot of the configuration at $t$ = 100 ns for p-THPP-PEG. The BIOCH and p-THPP molecules are shown in yellow as a licorice representation, while PEG chains are shown in orange. POPC lipids are depicted as sticks and colored as follows: blue, nitrogen; brown, phosphate; red, oxygen; and cyan, hydrocarbon chains. For clarity, water molecules are not shown.

found in our previous papers.[30,31] For water, we employed the TIP3P model, which is compatible with the OPLS parametrization.[32] Prior to the MD simulations, the steepest-descent algorithm was used to minimize the energy of the initial structure. The simulations were performed using the GROMACS software package.[33] Periodic boundary conditions were used in all three directions. The linear constraint solver (LINCS)[34] algorithm was used to preserve covalent bond lengths. The time step was set to 2 fs, and the simulations were carried out at constant pressure (1 bar) and temperature (300 K). The temperature and the pressure were controlled using the Nosé–Hoover[35] thermostat and the Parrinello–Rahman[36] barostat, respectively. For pressure, we used a semi-isotropic control in the simulations with a membrane and an isotropic control in the simulations without a membrane. In the simulations with a membrane, the temperatures of the solute and the solvent were controlled independently. The Lennard-Jones interactions were cut off at 1.0 nm, and for the electrostatic interactions, we employed the particle mesh Ewald method.[37]

Standard errors given for all numerical values in the paper were estimated using block analysis described previously.[38]

## 3. RESULTS

**3.1. The Partitioning of the Studied Molecules and Their PEGylated Derivatives Largely Depends on the Amount of Salt.** We first considered the location of the non-pegylated BIOCH and p-THPP inside the POPC membrane. Four molecules of BIOCH or p-THPP were initially placed at different positions with different orientations inside a membrane or in the aqueous phase (Figure 2A and D). Trajectories of the center of mass of BIOCH and p-THPP along the bilayer normal in the POPC membrane are presented in Figure S1 in the Supporting Information). The horizontal blue line on the plots shows the average position of the nitrogen atoms in the choline groups, and the red line, the position of the carbonyl oxygen atoms of the lipids. We found that, in the case of BIOCH, two molecules, which were initially placed in the hydrophobic center of the POPC membrane, migrated in 10–20 ns to the region near the carbonyl groups of POPC and remained there for the rest of the simulation time. In a similar manner, the two remaining molecules initially inserted into the aqueous phase diffused within 10 ns to the same location.

The p-THPP molecules exhibited similar behavior. Initially, three molecules of p-THPP were placed inside the POPC membrane, close to the center of the lipid bilayer. The remaining molecule was situated in a water phase, as shown in Figure 2D. Within 40 ns, the molecules moved from the center of the membrane toward the carbonyl groups of lipids, and remained there until the end of the simulations. p-THPP molecules initially placed in the water phase entered the lipid bilayer within the first 20 ns and stayed close to the region of the carbonyl groups of lipids. The localization of all non-PEGylated p-THPP and BIOCH molecules in the POPC membrane after 200 ns of simulation is visualized in Figure 2B and E.

Next, we considered the behavior of the PEGylated compounds in the presence of the lipid bilayer. In the case of p-THPP-PEG, we observed that in all simulations (with or without salt) the entire PEGylated compound stayed in the water phase (see snapshots in Figure 2F and Figure S1, Supporting Information). Similarly, the BIOCH-PEG molecule had no tendency to enter into the lipid membrane and it remained in the aqueous phase (Figure 2C). However, in the system without salt, the BIOCH-PEG molecule was able to move from the aqueous phase toward the membrane–water interface with the PEG chain interacting with both water and lipids. The subsequent stages of the process showing the BIOCH-PEG molecules' entrance into the bilayer are visualized in Figure 3. Parts A and B of Figure 3 show the BIOCH-PEG

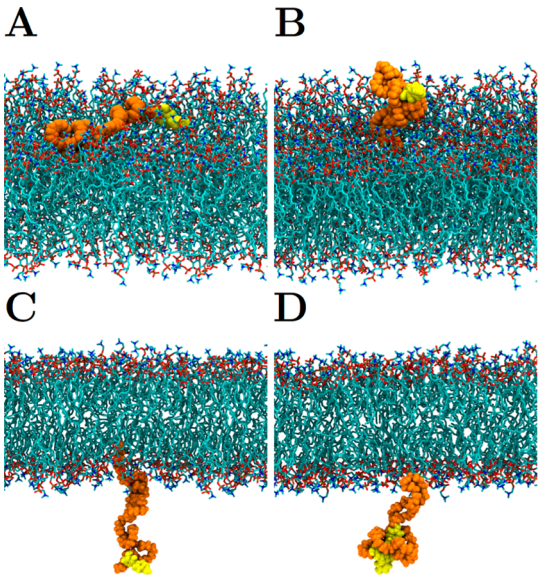


**Figure 3.** (A) A snapshot of BIOCH-PEG on a lipid bilayer after 1000 ns simulation without salt. (B, C) Two snapshots of BIOCH-PEG in systems without salt during BIOCH entry into a bilayer. (D) A snapshot of p-THPP-PEG in a system with salt showing that the PEG loop temporarily interacts with lipids. The BIOCH and p-THPP molecules are shown in yellow as a licorice representation, PEG chains in orange, and POPC lipids as sticks and colored as follows: blue, nitrogen; brown, phosphate; red, oxygen; and cyan, hydrocarbon chains. For clarity, water molecules are not shown.


dx.doi.org/10.1021/jp4105745 | J. Phys. Chem. B 2014, 118, 144–151

molecule fully adsorbed to the lipids, and Figure 3C shows an initial stage of adsorption, when a single PEG loop enters the lipid headgroup region. Figure 3D depicts a similar event of a single PEG loop entering the lipids in the system simulated with salt. This event, however, did not lead to full adsorption of the molecule at the lipid headgroup region. The trajectory of the center of mass of BIOCH-PEG in the POPC membrane without NaCl is presented in Figure S2 in the Supporting Information. BIOCH-PEG in the system without salt entered the membrane after a relatively long time of nearly 400 ns. Additionally, an animation of the BIOCH-PEG entrance into the lipid bilayer in the system without NaCl is also available in the Supporting Information.

To gain additional quantitative information regarding the localizations of all the studied molecules in the POPC membrane, we calculated the mass density profiles along the bilayer normal ($z$-coordinate) of the selected lipid headgroup atoms, the PEG chain, BIOCH, and p-THPP (Figure 4). Figure

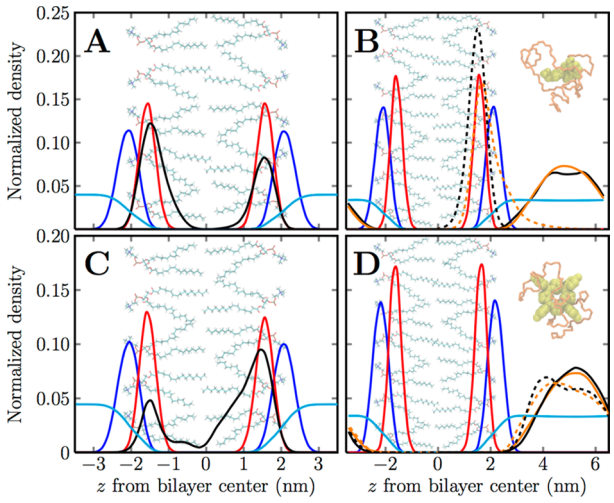


**Figure 4.** Mass density profiles of (A) BIOCH, (B) BIOCH-PEG, (C) p-THPP, (D) p-THPP-PEG, and the selected POPC atoms along the bilayer normal. The profiles are colored as follows: lipid nitrogen atoms (blue), lipid carbonyl oxygen atoms (red), water (light blue), BIOCH or p-THPP (black), and PEG (orange). Full/dashed lines show the results obtained in the simulations with/without salt, respectively. Profiles are averaged over all replicas. Profiles for the case of systems with and without salt are computed over the final 100 and 500 ns of trajectories, respectively.

4A shows that the non-pegylated BIOCH is located preferentially slightly below the average position of the carbonyl groups of the acyl chains of the POPC lipid, and the maximum of the density profile is at a distance of 1.49 nm from the bilayer center.

The location of non-pegylated p-THPP molecules in the bilayer is more complex and is characterized by two different preferred positions. Its profile has a maximum at 1.51 nm from the bilayer center and is strongly overlapped by the profiles of the lipid carbonyl groups. The second, deeper position is at 0.81 nm from the bilayer center. This behavior makes p-THPP different from hematoporphyrin, the location of which is characterized by a single preferred position at 1.7 nm from the bilayer center.[39]

The mass density profiles of BIOCH-PEG and p-THPP-PEG (Figure 4B and D) in the systems with NaCl show very limited overlap with the membrane, indicating that the PEGylated molecules do not penetrate beyond the depth of the nitrogen atoms in the bilayer. For the case of p-THPP-PEG in the system without salt, we did not observe the entrance of the molecule into the membrane; however, the density profiles changed their shapes with the maxima of distributions shifted toward the membrane. This means that the pegylated porphyrin can get closer to the membrane as compared to the system with salt. For the case of BIOCH-PEG simulated without salt, we observed that the BIOCH moiety is located almost at the same position as the native molecule (1.5 nm from the bilayer center), while the PEG chain situates at the water−membrane interface.

**3.2. Time Development of the Number of Contacts Shows the Binding Processes to Be Slow, Taking Place in up to Hundreds of Nanoseconds.** To evaluate direct interactions between the lipid bilayer and the studied molecules, we calculated the number of contacts between BIOCH/p-THPP molecules and lipids and PEG chains and lipids. It was assumed that a contact occured when the distance between atoms of the lipid and the studied molecule was smaller than 0.325 nm, which corresponds to the van der Waals radii of the carbon atoms. The time development of the number of contacts is shown in Figure 5.

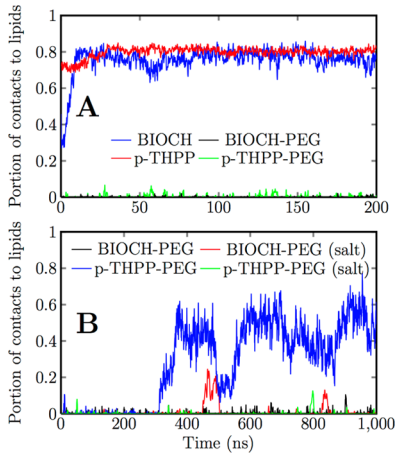


**Figure 5.** (A) Time development of the number of contacts between lipids and p-THPP (red), BIOCH (blue), p-THPP-PEG (green) (here PEG not included in analysis), and BIOCH-PEG (black) (PEG not included) in the simulations with salt, divided by all contacts between drug and surrounding molecules (lipids, water, and PEG). The number of contacts with p-THPP-PEG and BIOCH-PEG is very low. (B) Time development of the number of contacts between lipids and the PEG chain in p-THPP-PEG with salt (green) and without salt (black), and in BIOCH-PEG with salt (red) and without salt (blue) divided by all contacts between PEG and surrounding molecules.

As shown in Figure 5A, a negligible number of contacts was found for the moiety of the PEGylated molecules (orange and black lines) in the simulations performed in the presence of salt. The contacts occurred only for short periods of time (1−10 ns). For the case of the non-pegylated BIOCH or p-THPP (Figure 5A, blue and red lines), the number of contacts was approximately similar and remained constant after the molecules had entered the POPC bilayer. The observed difference is due to a different number of atoms in the structure of both molecules (the total number of atoms in BIOCH and p-THPP is 33 and 82, respectively).


dx.doi.org/10.1021/jp4105745 | J. Phys. Chem. B 2014, 118, 144−151

For all cases of PEGylated molecules, the number of contacts between PEG and lipid (Figure 5B) is considerably higher than the number of direct contacts between the BIOCH and p-THPP moieties of PEGylated molecules and lipids (Figure 5A). This is not surprising as the PEG chain wraps the functionalized molecule and forms an outer corona for the entire compound, as was demonstrated in Figure 3. Furthermore, Figure 5B clearly shows an effect of NaCl on the interaction of PEG with the membrane. From both PEGylated molecules, only BIOCH-PEG in the system without salt (blue line) was able to enter the POPC bilayer. Moreover, two large peaks for BIOCH-PEG in the system with salt (red line) are observed, which indicates that the PEG loops enter and leave the membrane for periods of the order of 10 ns. A snapshot illustrating such an event is shown in Figure 3D.

**3.3. Structure of PEGylated Compounds.** To elucidate the conformation of the polymer chain attached to the drug molecule, simulations of p-THPP-PEG and BIOCH-PEG in the aqueous solution were performed. Figure 6 shows the snapshots taken at 100 ns of the simulations. As clearly seen, the polymer chain surrounds the attached drug molecule, both in the system containing salt and without it.

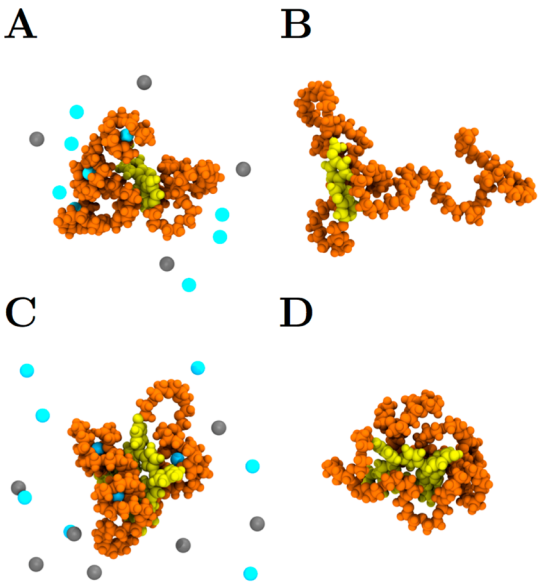


**Figure 6.** Snapshots of the systems in the aqueous solution taken after 100 ns of the simulation for (A) BIOCH-PEG with salt and (B) without it and (C) p-THPP-PEG with salt and (D) without it. The BIOCH and p-THPP molecules are shown in yellow as a licorice representation, while PEG chains are depicted in orange. $Cl^-$ and $Na^+$ ions are presented as gray and cyan spheres, respectively. For clarity, water molecules are not shown.

We calculated the radius of gyration ($R_g$) of the whole compound and the solvent accessible surface area (SASA) as a % of the total area covered by PEG of p-THPP and BIOCH molecules. The calculated values of $R_g$ and SASA for the simulation of the pegylated compounds in water are given in Table 2 and shown in Figure S3 (Supporting Information). The results indicate that p-THPP molecules are covered by PEG to a greater extent than BIOCH, and that the $R_g$ values for p-THPP are smaller. What is striking is that the standard deviation of $R_g$ is much smaller for the case of p-THPP-PEG, indicating that the whole conjugate is more compact and therefore has less degrees of freedom for dynamic fluctuations.

**Table 2. Radius of Gyration ($R_g$) and Solvent Accessible Surface Area (SASA) with Standard Deviation (SD) and Standard Error Estimates (SE)**

| | $R_g$ (nm) | SD | SE | SASA (%) | SD | SE |
|---|---|---|---|---|---|---|
| BIOCH-PEG (with salt) | 0.98 | 0.14 | 0.0084 | 0.45 | 0.16 | 0.010 |
| BIOCH-PEG (without salt) | 1.05 | 0.19 | 0.016 | 0.41 | 0.18 | 0.016 |
| p-THPP-PEG (with salt) | 0.91 | 0.06 | 0.0026 | 0.54 | 0.06 | 0.0037 |
| p-THPP-PEG (without salt) | 0.93 | 0.07 | 0.0038 | 0.57 | 0.08 | 0.0070 |

The presence of salt affects the structure of the compound by decreasing both $R_g$ as well as the standard deviation. Our results for the SASA for each system show that salt affects the two molecules in a different fashion: when salt is present, the coverage of p-THPP by PEG is decreased, while for the case of BIOCH it is increased.

**3.4. Role of Pegylation in Electrostatic Potential, Water Ordering, and Interaction with Ions.** To better understand interactions between the PEGylated molecules and the membrane, we calculated the electrostatic potential radially from the molecules' center of mass, following the method described by Heikkila et al.[40] The results are shown in Figure 7.

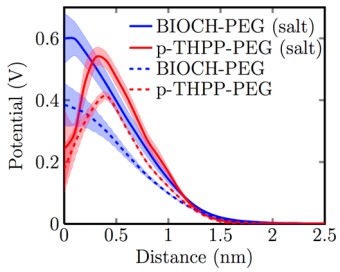


**Figure 7.** Electrostatic potentials calculated radially from the center of mass of the whole BIOCH-PEG (blue lines) and p-THPP-PEG (red lines) in systems with salt (solid lines) and without salt (dashed lines). Blue and red shades represent the standard deviations calculated from independent runs.

The profiles indicate that there is a positive potential barrier around the PEGylated molecules. Similarly, a positive potential barrier exists around lipid bilayers, as shown in numerous previous studies (e.g., ref 23) and Figure S4 in the Supporting Information; thus, PEGylated molecules and lipid bilayers experience electrostatic repulsive interactions.

It is well established that PEG interacts strongly with $Na^+$ ions.[30,41] Strong interactions of $Na^+$ with lipid bilayers composed of phosphatidylcholines are also well established.[24] To evaluate these interactions in our model system, we calculated the number of $Na^+$ ions bonded to PEG and lipid oxygen atoms. In our calculation, we used a distance criterion between $Na^+$ ions and PEG oxygen atoms of 0.350 nm.[23] We observed that ~2.5−3 ions are bonded with the PEG chain and the majority of the remaining ions are bonded to the membrane. The extent of this binding is in agreement with our previously published results.[22] At the same time, $Cl^-$ ions did not bind strongly with either PEG or the lipid bilayer. This allows us to expect that both PEG and the lipid bilayer carry a net positive charge that is, in part, responsible for the repulsive interactions between the pegylated drugs and the lipid bilayer


dx.doi.org/10.1021/jp4105745 | J. Phys. Chem. B 2014, 118, 144−151

in the presence of salt. A comparison of the electrostatic profiles around p-THPP-PEG and BIOCH-PEG simulated in a box of water with and without salt (Figure 7) showed that in the systems with salt the electrostatic potential is slightly higher, at about 0.15−0.2 V.

## 4. DISCUSSION

In this study, we considered how the attachment of a PEG chain to drug molecules (PEGylated drug molecules p-THPP and BIOCH) affects their behavior in aqueous solution. Also, we clarified the effect of this PEGylation on the drugs' entrance into biomembranes. The polymer length was chosen to be 45 units, which corresponds to a molecular weight of about 2000 Da. This molecular weight was previously shown as the most effective in a biological application of the PEGylated porphyrins.[13]

Generally, the conformation of a polymer chain attached to a small organic molecule is relatively poorly recognized in the literature. Therefore, we first simulated PEGylated molecules in an aqueous solution at physiological salt concentration and in the absence of salt. Our MD simulations showed a clear result: the PEG chain is wrapped around the moiety molecules (Figure 6). However, compactness of the polymer−drug conjugate is dependent on the chemical structure of the drug and the presence of salt. Although the BIOCH molecule is smaller (~1.28 nm in length and ~0.4 nm in width) in comparison to p-THPP (that is a symmetrical molecule with a diagonal of 1.8 nm), the radius of gyration of BIOCH-PEG is higher than that of the porphyrin conjugate (Table 2). In our previous paper, we showed that a more hydrophobic molecule has a stronger interaction with PEG, since this polymer is not completely hydrophilic. This interaction is lipophilic in nature; the non-polar $(CH_2)_2$ groups of the PEG chain interact with the non-polar surface of the molecule. Hydrophobicity of a given compound can be quantified using so-called lipophilicity parameters. One of the most widely used lipophilicity parameters is conveniently defined as the ratio of concentrations of the compound, as a neutral molecule, in *n*-octanol and aqueous phases ($P$) and used in the logarithmic form (log $P$).[42] Thus, log $P$ describes the affinity of the compound to the hydrophobic environment. For BIOCH, a log $P$ value of 2.007 has been reported,[43] whereas, for p-THPP, we predicted log $P$ to be 6.88 using an ALOGPS 2.1 program.[44] Thus, it is expected that the interaction between the porphyrin and PEG is stronger than that between PEG and BIOCH. As a result, the less hydrophilic porphyrin is more densely wrapped with the PEG chain than BIOCH.

We found some evidence from the MD simulations that the presence of salt at a physiological level changes the effective interactions between PEG and the attached molecules. The slight reduction of the $R_g$ values was observed in the systems containing salt, indicating that PEG is more contracted. Meanwhile, the portion of the surface area of the molecule covered by PEG (the remainder being exposed to the solvent) in the presence of salt in the case of p-THPP decreased and increased for BIOCH. These facts can be explained taking into account complexation of $Na^+$ cations by PEG chains.

Our simulation results are in line with experimental findings. Behavior of the PEGylated porphyrins, also p-THPP-PEG, in an aqueous solution has been studied using several experimental methods.[5] It has been shown that PEGylated porphyrins form polymer clusters (aggregates) in an aqueous solution. Through quenching the porphyrin chromophore fluorescence with potassium iodide, it has been shown that the porphyrin chromophores are localized within the PEG clusters. This experiment is in agreement with the effect of PEG as a steric mechanism; the polymer chain surrounds the porphyrin chromophore and prevents the collisions with the quencher molecules. Moreover, observations with atomic force microscopy (AFM) reveal that the apparent size of the PEGylated porphyrins in aqueous solution is significantly greater than that in the dry state. Thus, hydration of the PEG units will significantly increase the volume of the clusters in solution. Studies of PEG in solution have shown PEG typically binds 2−3 water molecules per ethylene oxide unit.[45] The interaction of the PEG chain with water results in the formation of a fixed layer of associated water molecules around the macromolecule.

There are several experimental pieces of evidence confirming that the free molecules of p-THPP and BIOCH can interact with a lipid bilayer. The fluorescence and UV absorption methods have been used to estimate binding of these compounds to liposomes. A so-called "binding constant" ($K_b$) of the drugs to a lipid bilayer was determined. $K_b$ is an experimental parameter, which indicates the affinity of a given compound to partition into a lipid membrane. As expected, the more lipophilic p-THPP is characterized by a relatively high $K_b$ value of 105 ± 35 mL/mg,[5] whereas for the more hydrophilic BIOCH this value is equal to 21.3 ± 3.8 mL/mg (see the Supporting Information).

We performed MD simulations of p-THPP and BIOCH, in both their native forms and functionalized with PEG, in the vicinity of a lipid bilayer. For the case of the molecules functionalized with PEG, we considered the effect of salt (NaCl) at the physiological concentration. In the simulations of p-THPP and BIOCH without attached PEG chain, we observed that the p-THPP molecules originally located in the aqueous phase entered the membrane (hydrocarbon) core within the first 40 ns of the simulations. A similar behavior was observed for hematoporphyrin in our previous publication.[39] The shape of the density profile of p-THPP, however, indicates two preferential locations within the membrane: one closer to the water−membrane interface and the second deeper within the membrane, at distances of 1.5 and 0.8 nm from the membrane center, respectively. For the case of non-PEGylated BIOCH, we observed a preferential location at the membrane−water interface, similar to numerous small compounds of amphipathic nature, e.g., neurotransmitters[46] and antibiotics.[47]

Functionalization of drug molecules affects their interactions with lipid bilayers by preventing them from entering the membrane, or by slowing down this process. The only case in which we observed entering of the PEGylated molecule (BIOCH-PEG) into the lipid bilayer occurred after 400 ns of the MD simulation.

The MD simulation results are consistent with experimental studies on interaction between the PEGylated p-THPP and the phospholipid membrane.[5] A fluorescence method has been used to estimate binding of the porphyrin chromophore to a lipid membrane. These results have demonstrated that the presence of the PEG chain has a significant effect on the binding constant of the porphyrin chromophore to a lipid bilayer. It was shown that the covalent attachment of PEG with a length of 45 units to the p-THPP ring caused a 9-fold decrease in the value of $K_b$.[5] Thus, the PEGylated porphyrin shows a considerably lower affinity to incorporate into a lipid membrane. In the simulations presented in this study, we did


dx.doi.org/10.1021/jp4105745 | J. Phys. Chem. B 2014, 118, 144−151

not see p-THPP-PEG entering the lipid bilayer, although our results do not exclude it. Our results for the SASA of p-THPP showed that a large portion of the hydrophobic surface is exposed to the water; thus, there are opportunities for the molecule to locate to the membrane. It is possible that due to the limitation of time scale in the current MD simulations we did not observe that phenomenon.

Our study has also demonstrated that $Na^+$ ions play a key role in modifying the interactions between membranes and PEGylated compounds. We observed that, in the systems containing salt, the PEGylated molecules remained in the aqueous phase, and the distance between the PEGylated compound and the lipid membrane was greater in comparison to the systems without salt. This indicates the occurrence of repulsive interactions between the PEGylated compounds and the lipid bilayer in the systems containing salt. It can be deduced that this interaction comes from electrostatic repulsions, with both lipid headgroups and PEG bound $Na^+$ ions thus becoming positively charged.

## 5. CONCLUSIONS

We used computer simulations to investigate the behavior of two PEGylated drugs, p-THPP and BIOCH, in the presence of a zwitterionic bilayer that was used as a model for the mammalian cellular membrane. In agreement with experiments, we found that the attachment of the polymer chain prevents or significantly delays the entering of the drug moiety to the lipid bilayer. The main reason for the lower affinity to the membranes is related to the wrapping of the attached molecule by the PEG chain; as a result, a corona is formed around the drug by the polymer. Our studies, however, showed important differences in the behavior of the PEGylated p-THPP and BIOCH, which most likely affects its interactions with membranes. We observed that BIOCH is more exposed to the water than porphyrin and that the PEG chain is less compact. Thus, interactions between BIOCH and the membrane are more likely than those for p-THPP. The protective or "stealth" properties imparted on the drug through PEGylation are the result of the barrier PEG creates between the drug and a cell membrane. Additionally, we see evidence of the presence of the electrostatic repulsion between PEGylated drugs and a lipid bilayer, both positively charged at a physiological level of the sodium cations. These observations may be important for understanding the behavior of PEGylated drugs in the bloodstream.

## ■ ASSOCIATED CONTENT

### Supporting Information

Animation of BIOCH-PEG in a simulation without salt showing the molecules' entry into a bilayer. Trajectories of the center of mass of BIOCH, p-THPP, BIOCH-PEG, and p-THPP-PEG. Trajectories of the center of mass of BIOCH-PEG and p-THPP-PEG in systems without salt. Histograms of the fraction of the drug surface covered by PEG. Electrostatic potentials along the bilayer normal in POPC membrane with salt and without salt. Determination of the binding constant for BIOCH. This material is available free of charge via the Internet at http://pubs.acs.org.

## ■ AUTHOR INFORMATION

### Corresponding Authors

*Phone: +48 12 6632020. Fax: +48 12 6340515. E-mail: kepczyns@chemia.uj.edu.pl (M.K.).

*Phone: +358 40 198 1010. Fax: +358 3 3115 3015. E-mail: tomasz.rog@gmail.com (T.R.).

### Notes

The authors declare no competing financial interest.

## ■ ACKNOWLEDGMENTS

The project was carried out within the Foundation for Polish Science Team Programme cofinanced by the EU European Regional Development Fund, PolyMed, TEAM/2008-2/6. S.R., T.R., and I.V. wish to thank the Academy of Finland for financial support (Center of Excellence in Biomembrane Research), and I.V. thanks the European Research Council (Advanced Grant project CROWDED-PRO-LIPIDS). For computational resources, we wish to thank the CSC − IT Center for Science (Espoo, Finland).

## ■ REFERENCES

(1) Torchilin, V. P. Liposomes as Delivery Agents for Medical Imaging. *Mol. Med. Today* **1996**, *2*, 242−249.

(2) Olivier, J. C. Drug Transport to Brain with Targeted Nanoparticles. *NeuroRx* **2005**, *2*, 108−119.

(3) Veronese, F. M.; Pasut, G. PEGylation for Improving the Effectiveness of Therapeutic Biomolecules. *Drugs Today* **2009**, *45*, 687−695.

(4) Pasut, G.; Veronese, F. M. PEG Conjugates in Clinical Development or Use as Anticancer Agents: An Overview. *Adv. Drug Delivery Rev.* **2009**, *61*, 1177−1188.

(5) Nawalany, K.; Kozik, B.; Kepczynski, M.; Zapotoczny, S.; Kumorek, M.; Nowakowska, M.; Jachimska, B. Properties of Polyethylene Glycol Supported Tetraaryporphyrin in Aqueous Solution and its Interaction with Liposomal Membranes. *J. Phys. Chem. B* **2008**, *112*, 12231−12239.

(6) Moghimi, S. M.; Szebeni, J. Stealth Liposomes and Long Circulating Nanoparticles: Critical Issues in Pharmacokinetics, Opsonization and Protein-Binding Properties. *Prog. Lipid Res.* **2003**, *42*, 463−478.

(7) Yamaoka, T.; Tabata, Y.; Ikada, Y. Distribution and Tissue Uptake of Poly(Ethylene Glycol) with Different Molecular Weights After Intravenous Administration to Mice. *J. Pharm. Sci.* **1994**, *83*, 601−606.

(8) Webster, R.; Didier, E.; Harris, P.; Siegel, N.; Stadler, J.; Tilbury, L.; Smith, D. PEGylated Proteins: Evaluation of their Safety in the Absence of Definitive Metabolism Studies. *Drug Metab. Dispos.* **2007**, *35*, 12419/3160041.

(9) Hornung, R.; Fehr, M. K.; Monti-Frayne, J.; Krasieva, T. B.; Trommberg, B. J.; Berns, M. W.; Tadir, Y. Highly Selective Targeting of Ovarian Cancer with the Photosensitizer PEG-m-THPC in a Rat Model. *Photochem. Photobiol.* **1999**, *70*, 624−629.

(10) Grahn, M. F.; Giger, A.; McGuinness, A.; de Jode, M. L.; Stewart, J. C. M.; Ris, H.-B.; Altermatt, H. J.; Williams, N. S. mTHPC Polymer Conjugates: The in Vivo Photodynamic Activity of Four Candidate Compounds. *Lasers Med. Sci.* **1999**, *14*, 40−46.

(11) Lottner, C.; Bart, K.-C.; Bernhardt, G.; Brunner, H. Soluble Tetraarylporphyrin-Platinum Conjugates as Cytotoxic and Phototoxic Antitumor Agents. *J. Med. Chem.* **2002**, *45*, 2079−2089.

(12) Lottner, C.; Knuechel, R.; Bernhardt, G.; Brunner, H. Distribution and Subcellular Localization of a Water-Soluble Hematoporphyrin-Platinum(II) Complex in Human Bladder Cancer Cells. *Cancer Lett.* **2004**, *215*, 167−177.

(13) Nawalany, K.; Rusin, A.; Kepczynski, M.; Filipczak, P.; Kumorek, M.; Kozik, B.; Weitman, H.; Ehrenberg, B.; Krawczyk, Z.; Nowakowska, M. Novel Nanostructural Photosensitizers for Photodynamic Therapy: *In Vitro* Studies. *Int. J. Pharm.* **2012**, *430*, 129−140.

(14) Zhang, J. H.; Du, F. P.; Peng, B.; Lu, R. H.; Gao, H. X.; Zhou, Z. Q. Structure, Electronic Properties, and Radical Scavenging Mechanisms of Daidzein, Genistein, Formononetin, and Biochanin A: A

Density Functional Study. *J. Mol. Structure: THEOCHEM* **2010**, *955*, 1−6.
(15) Cowan, M. M. Plant products as antimicrobial agents. *Clin. Microbiol. Rev.* **1999**, *12*, 564−582.
(16) Hsu, J.-T.; Hung, H.-C.; Chen, C.-J.; Hsu, W.-L.; Ying, C. Effects of the Dietary Phytoestrogen Biochanin A on Cell Growth in the Mammary Carcinoma Cell Line MCF-7. *J. Nutr. Biochem.* **1999**, *10*, 510−517.
(17) Rusin, A.; Krawczyk, Z.; Grynkiewicz, G.; Gogler, A.; Zawisza-Puchałka, J.; Szeja, W. Synthetic Derivatives of Genistein, their Properties and Possible Applications. *Acta Biochim. Pol.* **2010**, *57*, 23−34.
(18) Uckun, F. M.; Narla, R. K.; Zeren, T.; Yanishevski, Y.; Myers, D. E.; Waurzyniak, B.; Ek, O.; Schneider, E.; Messinger, Y.; Chelstrom, L. M.; et al. In Vivo Toxicity, Pharmacokinetics, and Anticancer Activity of Genistein Linked to Recombinant Human Epidermal Growth Factor. *Clin. Cancer Res.* **1998**, *4*, 1125−1134.
(19) Lewis, P. T.; Wahala, K.; Hoikkala, A.; Mutikainen, I.; he Meng, Q.; Lewis, P. T.; Wa, K.; Adlercreutz, H.; Tikkanen, M. J. Synthesis of Antioxidant Isoflavone Fatty Acid Esters. *Tetrahedron* **2000**, *56*, 7805−7810.
(20) Polkowski, K.; Popiołkiewicz, J.; Krzeczyn, P.; Pucko, W.; Zegrocka-Stendel, O.; Boryski, J.; Skierski, J. S.; Mazurek, A. P.; Grynkiewicz, G. Cytostatic and Cytotoxic Activity of Synthetic Genistein Glycosides Against Human Cancer Cell Lines. *Cancer Lett.* **2004**, *203*, 59−69.
(21) Vasselin, D. A.; Westwell, A. D.; Matthews, C. S.; Bradshaw, T. D.; Stevens, M. F. G. Structural Studies on Bioactive Compounds. 401. Synthesis and Biological Properties of Fluoro-, Methoxyl-, and Amino-Substituted 3-phenyl-4H-1-benzopyran-4-ones and a Comparison of their Antitumor Activities with the Activities of Related 2-phenyl-benzot. *J. Med. Chem.* **2006**, *49*, 3973−3981.
(22) Moghimi, S. M.; Hunter, A. C.; Murray, J. C. Long-Circulating and Target-Specific Nanoparticles: Theory to Practice. *Pharmacol. Rev.* **2001**, *53*, 283−318.
(23) Li, Y.-C.; Rissanen, S.; Stepniewski, M.; Cramariuc, O.; Róg, T.; Mirza, S.; Xhaard, H.; Wytrwal, M.; Kepczynski, M.; Bunker, A. Study of Interaction Between PEG Carrier and three Relevant Drug Molecules: Piroxicam, Paclitaxel, and Hematoporphyrin. *J. Phys. Chem. B* **2012**, *116*, 7334−7341.
(24) Stepniewski, M.; Bunker, A.; Pasenkiewicz-Gierula, M.; Karttunen, M.; Róg, T. Effects of the Lipid Bilayer Phase State on the Water Membrane Interface. *J. Phys. Chem. B* **2010**, *114*, 11784−11792.
(25) Jorgensen, W. L.; Maxwell, D. S.; Tirado-Rives, J. Development and Testing of the OPLS All-Atom Force Field on Conformational Energetics and Properties of Organic Liquids. *J. Am. Chem. Soc.* **1996**, *118*, 11225−11236.
(26) Rizzo, R. C.; Jorgensen, W. L. OPLS All-Atom Model for Amines: Resolution of the Amine Hydration Problem. *J. Am. Chem. Soc.* **1999**, *121*, 4827−4836.
(27) Price, M. L.; Ostrovsky, D.; Jorgensen, W. L. Gas-Phase and Liquid-State Properties of Esters, Nitriles, and Nitro Compounds with the OPLS-AA Force Field. *J. Comput. Chem.* **2001**, *22*, 1340−1352.
(28) Kaminski, G. A.; Friesner, R. A.; Tirado- Rives, J.; Jorgensen, W. L. Evaluation and Reparametrization of the OPLS-AA Force Field for Proteins via Comparison with Accurate Quantum Chemical Calculations on Peptides. *J. Phys. Chem. B* **2001**, *105*, 6474−6487.
(29) Siu, S. W. I.; Pluhackova, K.; Böckmann, R. A. Optimization of the OPLS-AA Force Field for Long Hydrocarbons. *J. Chem. Theory Comput.* **2012**, *8*, 1459−1470.
(30) Sepniewski, M.; Pasenkiewicz-Gierula, M.; Rog, T.; Danne, R.; Orlowski, A.; Karttunen, M.; Urtti, A.; Yliperttula, M.; Vuorimaa, E.; Bunker, A. Study of PEGylated Lipid Layers as a Model for PEGylated Liposome Surfaces: Molecular Dynamics Simulation and Langmuir Monolayer Studies. *Langmuir* **2011**, *27*, 7788−7798.
(31) Orłowski, A.; St-Pierre, J.-F.; Magarkar, A.; Bunker, A.; Pasenkiewicz-Gierula, M.; Vattulainen, I.; Róg, T. Properties of the Membrane Binding Component of Catechol-O-methyltransferase Revealed by Atomistic Molecular Dynamics Simulations. *J. Phys. Chem. B* **2011**, *115*, 13541−13550.
(32) Jorgensen, W. L.; Chandrasekhar, J.; Madura, J. D.; Impey, R. W.; Klein, M. L. Comparison of Simple Potential Functions for Simulating Liquid Water. *J. Chem. Phys.* **1983**, *79*, 926−935.
(33) Hess, B.; Kutzner, C.; van der Spoel, D.; Lindahl, E. GROMACS 4: Algorithms for Highly Efficient, Load-Balanced, and Scalable Molecular Simulation. *J. Chem. Theory Comput.* **2008**, *4*, 435−447.
(34) Hess, B.; Bekker, H.; Berendsen, H. J. C.; Fraaije, J. G. E. M. LINCS: A Linear Constraint Solver for Molecular Simulations. *J. Comput. Chem.* **1997**, *18*, 1463−1472.
(35) Nose, S. A Unified Formulation of the Constant Temperature Molecular Dynamics Methods. *J. Chem. Phys.* **1984**, *81*, 511−519.
(36) Parrinello, M.; Rahman, A. Polymorphic Transitions in Single Crystals: A New Molecular Dynamics Method. *J. Appl. Phys.* **1981**, *52*, 7182−7190.
(37) Essman, U.; Perera, L.; Berkowitz, M. L.; Darden, H. L. T.; Pedersen, L. G. A Smooth Particle Mesh Ewald Method. *J. Phys. Chem.* **1995**, *103*, 8577−8592.
(38) Hess, B. Determining the Shear Viscosity of Model Liquids from Molecular Dynamics Simulations. *J. Chem. Phys.* **2002**, *116*, 209.
(39) Stępniewski, M.; Kepczynski, M.; Jamróz, D.; Nowakowska, M.; Rissanen, S.; Vattulainen, I.; Róg, T. Interaction of Hematoporphyrin with Lipid Bilayer. Molecular Dynamics Simulation Studies. *J. Phys. Chem. B* **2012**, *116*, 4889−4897.
(40) Heikkila, E.; Gurtovenko, A. A.; Martinez-Seara, H.; Hakkinen, H.; Vattulainen, I.; Akola, J. Atomistic Simulations of Functional Au144(SR)60 Gold Nanoparticles in Aqueous Environment. *J. Phys. Chem. C* **2012**, *116*, 9805−9815.
(41) Magarkar, A.; Karakas, E.; Stepniewski, M.; Róg, T.; Bunker, A. Molecular Dynamics Simulation of PEGylated Bilayer Interacting with Salt Ions: a Model of the Liposome Surface in the Bloodstream. *J. Phys. Chem. B* **2012**, *116*, 4212−4219.
(42) Kępczyński, M.; Pandian, R. P.; Smith, K. M.; Ehrenberg, B. Do Liposome-Binding Constants of Porphyrins Correlate with their Measured and Predicted Prtitioning Between Octanol and Water? *Photochem. Photobiol.* **2002**, *76*, 127−134.
(43) Gania-Pietrzak, B.; Hendrich, A. B.; Żugaj, J.; Michalak, K. Metabolic O-demethylation Does Not Alter the Influence of Isoflavones on the Biophysical Properties of Membranes and MRP1-like Protein Transport Activity. *Arch. Biochem. Biophys.* **2005**, *433*, 428−434.
(44) Tetko, I. V.; Gasteiger, J.; Todeschini, R.; Mauri, A.; Livingstone, D.; Ertl, P.; Palyulin, V. A.; Radchenko, E. V.; Zefirov, N. S.; Makarenko, A. S.; et al. Virtual Computational Chemistry Laboratory - Design and Description. *J. Comput.-Aided Mol. Des.* **2005**, *19*, 453−463.
(45) Roberts, M. J.; Bentley, M. D.; Harris, J. M. Chemistry for Peptide and Protein PEGylation. *Adv. Drug Delivery Rev.* **2002**, *54*, 459−476.
(46) Orłowski, A.; Bunker, A.; Pasenkiewicz-Gierula, M.; Vattulainen, I.; Männistö, P. T.; Róg, T. Strong Preferences of Dopamine and L-dopa Towards Lipid Head Group: Importance of Phosphatidylserine and its Implication for Neurotransmitters Metabolism. *J. Neurochem.* **2012**, *122*, 681−690.
(47) Cramariuc, O.; Rog, T.; Polishchuk, A. V.; Vattulainen, I. Molecular Dynamics Simulations Suggest a Mechanism for Translocation of Fluoroquinolones Across Lipid Membranes. *Biochim. Biophys. Acta* **2012**, *1818*, 2563−2571.